Journal of Civil Engineering
The Institution of Engineers, Bangladesh
Vol. CE 24, No. 1, 1996

STRAIN-INDUCED ANISOTROPY IN THE SMALL STRAIN STIFFNESS OF GRANULAR MATERIALS

E. Hoque[1], F. Tatsuoka[2] and S. Teachavorasinskun[3]

ABSTRACT : The conventional triaxial testing system has been modified to solve several major potential problems encountered in stress and strain measurements. Cyclic triaxial tests were performed on air-pluviated dry specimens of Toyoura and Ticino sands. The effects of 'induced strain' resulting from cyclic loading (or cyclic prestraining) was investigated on the deformation characteristics at relatively small strains, including the elastic parameter E_{max}- the maximum Young's modulus. The effects of aging before and after cyclic prestraining (CP) were also investigated. It was observed that the soil specimen becomes more anisotropic, may be called CP-induced anisotropy, in the small strain modulus as a result of CP.

KEY WORDS : Triaxial cyclic loading, prestraining, aging, local-strain anisotropy.

INTRODUCTION

A soil mass upon which a structure is founded often experiences cyclic loading caused by fluctuations in loading intensity. For instance, in the case of wave loading on offshore structures, traffic loading on pavements and heavy machine vibrations on foundations, the number of cyclic loading is very large although the magnitude of the non-constant component of loading is relatively small. The effects of a series of small seismic loading may also be included in this category. In such a case, the effects on the deformation characteristics of soil cannot be ignored in the design.

Effects of cyclic prestraining (CP) and consolidation time on the elastic modulus and some other deformation parameters at relatively small strains of less than, say 0.1%, of granular materials are still poorly understood. A large number of loading cycles with a high shear-strain amplitude increases the values of shear modulus and damping ratio of a clean sand, while the increase in the shear modulus and damping due to CP continues with the number of loading cycles during CP (Drnevich and Richart, 1970). The elastic shear modulus G_{max} for an aged in-situ sand deposit can be reproduced in the laboratory by applying an

1 Department of Civil Engineering, BUET, Dhaka-1000, Bangladesh
2 Department of Civil Engineering University of Tokyo
3 Department of Civil Engineering, International Institute of Technology, Thammasat University, Thailand.

appropriate amount of cyclic loading followed by consolidation for an appropriate period to an 'undisturbed' sample that may have been disturbed during sampling, transportation, etc. (Tokimatsu et al., 1986). However, some other researchers, Alarcon-Guzman et al. (1980) and De Alba et al. (1984), showed G_{max} of a clean sand is rather insensitive to CP. On the other hand, shear modulus increases noticeably with consolidation time even for a clean sand (Hardin and Drnevich, 1972; Tokimatsu et al., 1986).

This paper will describe the effects of CP as well as aging on some of the soil parameters in the light of the results from a comprehensive series of triaxial tests.

DESCRIPTION OF THE TESTING SYSTEM

The triaxial apparatus used in this study (Fig. 1) is one of the modified apparatuses which has been in use in the authors' laboratory at Institute of Industrial Science, University of Tokyo. Unlike many other conventional triaxial systems, it includes facilities for a) measurements of axial load by using a sensitive and rigid load cell installed within the triaxial cell (No. 1 in Fig. 1) to eliminate the effects of piston friction, b) automated anisotropic consolidation by controlling axial stress (σ_a) and radial stress (σ_r) independently, c) bedding-error-free 'on-sample' direct measurements of axial deformation by using local deformation transducers LDTs (No. 3) (Goto et al., 1991), and d) local measurements of radial deformations of dry specimen by using 3 pairs of proximity transducers mounted on an attachment system (No. 2).

One proximity transducer (No. 4) and one dial gage (No. 6) were also used to measure the displacements of the loading cap and the loading piston, respectively. Although external strains obtained from the above may include large effects of bedding error (Hoque et al., 1995; Jardine et al., 1984; Tatsuoka and Kohata, 1995; Tatsuoka et al., 1995), it was measured to cross-check conclusions which may be obtained from local strain measurements by using a pair of LDTs. Radial strains were measured at three heights (2.5-, 7.5- and 12.5-cm from the bottom) of a dry specimen assuming that radial strain distribution could be less uniform in the vertical direction compared with axial strain distribution. Two sets of proximeters, each set consisting of three, were fixed on a pair of two-direction micrometer tables (No. 7, Fig. 1) so that they can be effectively moved along the vertical and horizontal directions at any stage of the test if required; horizontal movement/shifting is often required when repeated loading test is performed, since such a test usually brings about large plastic deformation.

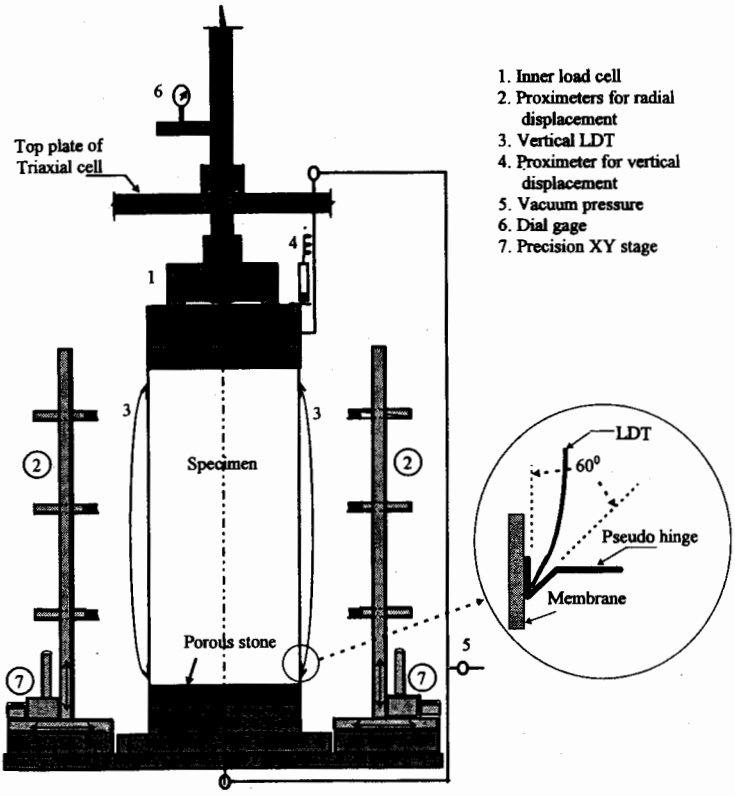

Fig 1. An instrumented triaxial apparatus used in the present study

Tests were performed by using a stress-controlled cyclic loading (CL) system. The system has two basic components: a static pressure component and a dynamic pressure component, both being fed into from a house pressure unit. The house pressure unit consists of (a) an air compressor, which supplies high air pressure; (b) a regulator, which based on the maximum pressure preset by an operator, provides constant house pressure from the air-compressor, and (C) an accumulator and filter tank unit, which filters and then accumulates the supplied air. The static pressure unit fed by a high pressure line (HPL) from the accumulator, supplies static pressure via a regulator to the lower chamber of a double-action Bellofram cylinder. On the other hand, dynamic pressure is controlled by an electro-pneumatic (E/P) transducer through its two inlets. One inlet is connected to a HPL from the accumulator. The other receives driving signals for cyclic loading from a control unit, an auto-function generator. The E/P transducer receives continuous signals, depending on the amplitude and frequency of a CL test as preset by the operator, from the function generator and converts it

accordingly into an equivalent pressure. Finally, the equivalent pressure after being amplified in volume by using another regulator (booster) is conveyed to the upper chamber of the Bellofram cylinder. A specimen is directly connected to the Bellofram cylinder through a loading piston. Any change in pressure, static or cyclic, in the Bellofram cyclinder results in the corresponding change in the axial stress of the specimen. The confining stress was applied by partial vacuum (No. 5).

Using a 12-bit 16 channel analogue-to-digital converter card, the data acquired by using transducers (1)~(4) is fed into a 16-bit micro-computer.

TEST PROCEDURE

A solid, cylindrical specimen of 7.5 cm in diameter and 15 cm in height, was reconstituted by raining sand particles through air into a split mold. Regular ends (i.e., non-lubricated ends using a porous stone) were used at both ends of the specimen. A partial vacuum of 0.1 kgf/cm^2 was applied. After dissembling the mold, a free-standing specimen, enclosed within a rubber membrane, was consolidated isotropically to pressure (σ_c) at which the specimen dimensions were measured before any instrumentation. Cyclic loading tests were then performed. In most of the tests, the neutral stress condition was isotropic.

Young's modulus was evaluated by applying small cyclic axial load for which the single-amplitude axial strain, $(\varepsilon_a)_{SA}$, was kept within 0.002%. The Young's modulus of a specimen of clean sand evaluated at this strain level is observed similar to that obtained by measuring body wave velocities (Jamiol Kowski et al., 1991; Tatsuoka and Kohata, 1995; Tatsuoka et al., 1995). So, this value can be considered to be the maximum Young's modulus which a soil element can exhibit in its current state. Therefore, the Young's modulus defined for the range will be called herein the maximum Young's modulus, E_{max}. Equivalent Young's moduli E_{eq} were evaluated from the response during a CL test performed at specific value of $(\varepsilon_a)_{SA}$. The range of $(\varepsilon_a)_{SA}$ was varied from around 0.001% to a value $(\varepsilon_a)_{SA.CP}$ at which cyclic prestraining was applied.

Cyclic loading, including CP, was applied symmetrically about an isotropic stress state. The loading frequency (f) for CP was 0.5 Hz, while it was 0.1 Hz for the CL tests performed for evaluating soil parameters. A prescribed number of cyclic loading was applied during CP at $(\varepsilon_a)_{SA.CP}$, which was varied in the range of 0.025~0.1% from a specimen to another.

TEST PROGRAM

Test program consisted of CL tests at various amplitudes to investigate the effects of cyclic prestraining (CP) on the maximum Young's modulus (E_{max}), the peak-to-peak scant Young's modulus (E_{eq}) and the tangent modulus along a CP-stress path. Effects of aging on E_{max} and E_{eq} were also investigated before and after CP for some specimens. Two types of test programs were employed in this investigation. In the first type (Group 1; Fig. 2a), the effects of CP and aging on some of the soil parameters were investigated; a specified number of loading cycles were

applied as CP at a single stage with a more-or-less constant $(\varepsilon_a)_{SA.CP}$. In the other type (Group 2; Fig. 2b), the effects of the degree of CP were investigated on E_{max}, E_{eq} and so on; the number of loading cycles and the amplitude $(\varepsilon_a)_{SA.CP}$ during CP were varied at multiple stages while increasing their values after each stage. The testing conditions is listed in Table 1. All tests were performed at dry state.

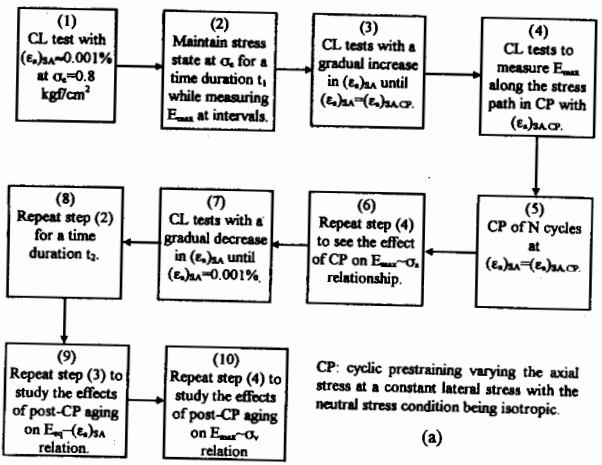

Fig 2. Block diagram of test program for test series : (a) Group 1 and (b) Group 2

Table 1. List of the Tests

Test Name /(group)	Change in $e_{0.8}$ or $e_{0.5}$	σ_c (kgf/cm²)	K σ_r/σ_a	$(\varepsilon_a)_{SA.CP}$ (%)	CP cycle (N)
T1/(1)	0.75~0.729	0.8	1	0.025	25000
T2/(1)	0.65~0.637	0.8	1	0.022	25000
TCC/(2)	0.707~0.701	0.5	1	0.029~0.031	15~68695
LTO/(2)	0.819~0.755	0.5	1	0.03~0.101	15~162935
TI/(2)	0.664~0.668	0.5	1	0.04~0.051	15~142000
HTC/(2)	0.701~0.690	0.8	1	0.02~0.035	300~163600
LHT/(2)	0.808~0.770	0.8	1	0.02~0.035	300~163600
TO/(2)	0.704~0.708	0.5	0.40	0.035~0.05	15~67335

TEST RESULTS

Most of the tests were performed on Toyoura sand, which is a fine-grained sand, quartz-dominant and sub-angular in grain shape. Some of the tests were performed on silica-dominant, sub-round Ticino sand. The physical properties are listed in Table 2.

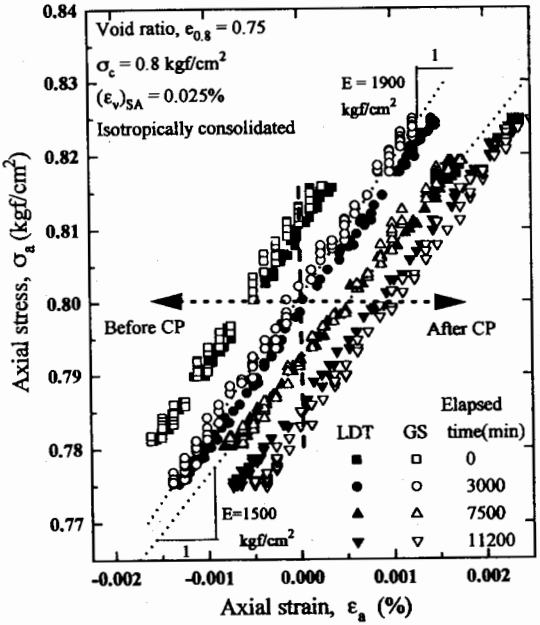

Fig 3a. $\sigma_a \sim \varepsilon_a$ responses of typical CL tests with $(\varepsilon_a)_{SA} \leq 0.002\%$ (1 kg f/cm^2 = 98 kpa)

Fig. 3a shows the typical axial stress (σ_a) and axial stain (ε_a) relationships obtained from four small-amplitude CL tests performed on a Toyoura sand specimen of void ratio $e_{0.8}$ = 0.75; note that the subscript of e indicates the value of consolation pressure, σ_c (kgf/cm^2), at which void ratio was measured initially. These responses are those obtained 'long before', 'immediately before', 'immediately after' and 'long after' CP application. The residual axial strain that occurred due to CP was 0.107% (extension), but this value was ignored in Figs. 2a and b. The elapsed time is defined as the cumulative time initialized at the beginning of the cyclic loading testing. The responses were essentially linear and recoverable with the slope after CP being slightly smaller than that before CP, indicating a negative influence of CP on the stiffness. The Young's moduli evaluated by using gap-senor (GS; No. 4 in Fig. 1) was slightly larger than the respective value by LDTs. This would be due to that the specimen was denser near both ends. The difference is, however, very small. Note that this trend is not general, but for a dense sample, the Young's modulus is

usually noticeably larger when based on local strains than external strains (Jardine et al., 1984; Tatsuoka and Kohata, 1995; Tatsuoka et al., 1995). The use of a local gage such as LDT is imperative in triaxial tests on a coarse grained material. In evaluating the maximum Young's modulus E_{max}, the single-amplitude axial strain, $(\varepsilon_a)_{SA}$, was less than 0.002%.

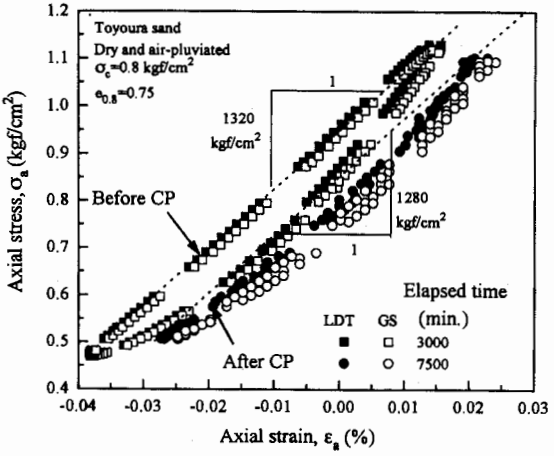

Fig 3b. $\sigma_a \sim \varepsilon_a$ responses of typical CL tests with $(\varepsilon_a)_{SA} = (\varepsilon_a)_{SA.cp}$(1kg f/cm^2 = 98 kpa)

Fig. 3b shows the typical σ_a~ε_a relationships obtained during prestraining cycles, 'immediately before' and 'immediately after' the application of a large amount of CP for the same specimen. It can be seen that although the hysteresis area and hence the damping ratio (not described in this paper) decreased drastically by CP, E_{eq} at or near $(\varepsilon_a)_{SA} = (\varepsilon_a)_{SA.cp}$ did not change noticeably.

Table 2. Test Materials

Sand	D_{10} (mm)	D_{50}(mm)	U_C	G_S	e_{max}	e_{min}
Toyoura	0.11	0.162	1.46	2.64	0.97	0.61
Ticino	0.32	0.502	1.33	2.68	0.96	0.59

Equivalent Young's modulus E_{eq}

Herein only the Young's moduli evaluated by using axial strains measured locally (with LDT) will be presented. Fig. 4a shows the effects of CP and post-straining long-term consolidation on the E_{eq}~log$(\varepsilon_a)_{SA}$ relation for an air-dried specimen having $e_{0.8}$=0.75. Due to CP, E_{eq} at a specific $(\varepsilon_a)_{SA}$ decreased except near and at the strain amplitude $(\varepsilon_a)_{SA.CP}$, with the maximum reduction (≈22%) at the smallest $(\varepsilon_a)_{SA}$. Partial recovery of stiffness from the damage due to CP was observed in the post-

straining consolidation period. The recovery in terms of the increment of E_{eq} was rather constant for the range of $(\varepsilon_a)_{SA}$ examined except near and at $(\varepsilon_a)_{SA.CP}$. The effects of CP and aging on the E_{max} value will be discussed later.

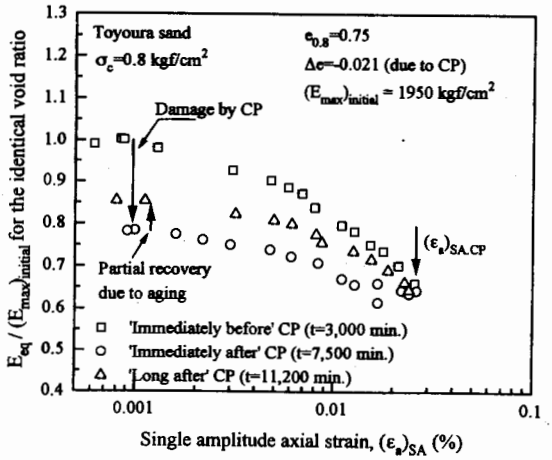

Fig 4a. E_{eq}~ Log $(\varepsilon_a)_{SA}$ variations at different times (1 kgf/cm^2 = 98 kPa)

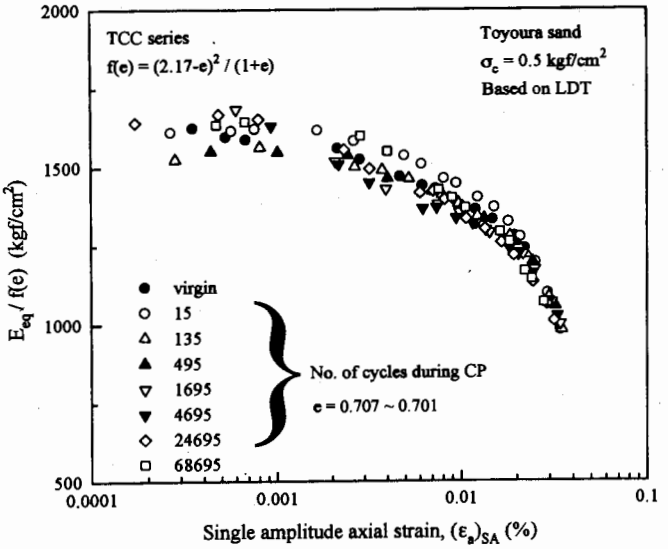

Fig 4b. E_{eq}~ Log $(\varepsilon_a)_{SA}$ variations at different degree of prestraining (1 kgf/cm^2 - 98 kPa)

It has been found from the results of many similar tests that the effects of CP on the E_{eq}~log$(\varepsilon_a)_{SA}$ relation is not consistent. Fig. 4b shows

the results from another series of tests, in which E_{eq}~log $(\varepsilon_a)_{SA}$ relations were evaluated after the application of various levels of CP (see Fig. 2b). Both $(\varepsilon_a)_{SA}$ and the number of loading cycle N during each CP stage were varied among stages; the former in the range of 0.029~0.0305% and N in the range of 1~68695. Note that N means the number of loading cycles during CP which was applied immediately before each E_{eq}~$(\varepsilon_a)_{SA}$ relation was evaluated; thus N is not an accumulated value. In this case, generally CP did not produce a remarkable influence on the decay curves; the values of E_{eq} at a given $(\varepsilon_a)_{SA}$ were varied within a narrow band.

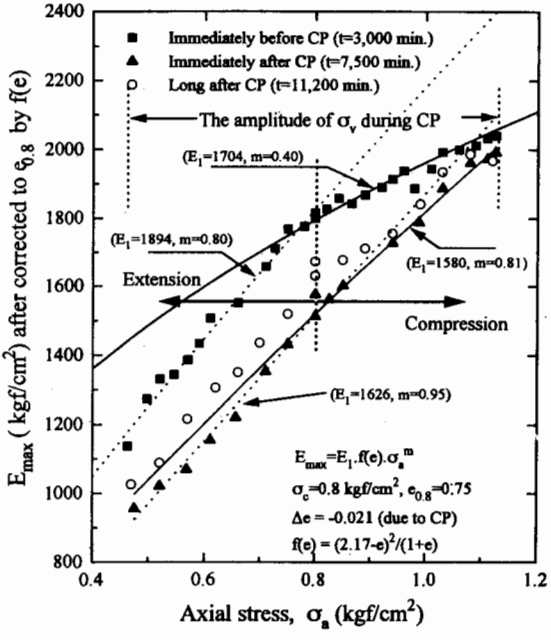

Fig 5. Variation of E_{max} along the stress path of CP cycle (1 kgf/cm² = 98 kPa)

Axial Stress-Dependency of E_{max}

Fig. 5 shows the relationship of the E_{max} value with axial stress (σ_a) for an air-dried specimen having void ratio $e_{0.8}$=0.75. The values of E_{max} were evaluated from the responses of small amplitude CL tests along the stress path applied in CP. Effects of CP and post-CP long-term consolidation on this relation were investigated. The values of E_{max} were measured while increasing σ_a, and have been corrected for e = 0.75 by using the function $f(e) = (2.17-e)^2/(1+e)$ to account for the change which occurred during the course of testing. Due to CP, the E_{max}~σ_a relation was rotated downward with a large reduction in E_{max} in the extension side while keeping E_{max} near the peak axial stress during CP nearly unchanged. This resulted in the decrease in the parameter E_1, where $E_{max} = E_1 \cdot f(e) \cdot \sigma_a^m$, while increasing the value of the exponent m. Elastic

parameters E_1 and m for events 'before CP' and 'after CP' are listed in Table 3; these parameters were evaluated separately for extension and compression stress-states from the respective E_{max}~σ_a relation. Both parameters depend generally on the fabric, the particle size, shape, angularity and orientation in a given mass and so on. Before CP, the elastic parameters E_1 and m in compression stress states differed noticeably from those in extension stress states— producing two distinct E_{max}~σ_a relations Flora et al. (1994). As at result of CP, on the other hand, the pair of E_1 and m were changed further noticeably compared to their respective values before CP. The Young's modulus E_{max} of a granular material depends essentially on the principal stress in the direction of the major principal strain increment for which the E_{max} value is defined. By this property, the elasticity of granular material becomes anisotropic under anisotropic stress conditions (i.e., stress state-induced anisotropy: Hoque et al., 1995; Hoque et al., 1996; Stokoe et al., 1991; Tatsuoka and Kohata, 1995). Therefore, the change in the exponent m implies a corresponding change in the value of $\sigma_a{}^m$— which, in turn, affects directly the stress-induced anisotropy characteristics. Thus, the specimen attained a new state of anisotropy, which may be called 'CP-induced anisotropy.' At this state, the corresponding values of E_1 and m obtained separately in extension and compression stress states became rather similar—exhibiting almost a unique E_{max}~σ_a relation with the value of exponent m close to unity. Although effects on E_1 of CP was not consistent (Fig. 4a and b), the behaviour 'CP-induced anisotropy' was observed in all other tests. On the other hand, partial recovery of E_{max} during post-CP long-term consolidation can also be observed, which was maximum at the smallest σ_a.

Table 3. Basic Elastic Parameters (1 kgf/cm² = 98 kPa)

	Compression state		Extension state	
	E_1 (kgf/cm²)	m	E_1 (kgf/cm²)	m
Before CP	1704	0.40	1894	0.80
After CP	1580	0.81	1626	0.95

Tangent Modulus E_{tan}

Fig. 6 shows the relationship between the tangent Young's modulus (E_{tan}) and the axial stress (σ_a) for the hysteresis curves shown in Fig. 3b. Variation of E_{max} (as shown in Fig. 5) along the CP stress cycle is also plotted for comparison. The values of E_{tan} during both reloading (σ_a increasing) and unloading (σ_a decreasing) phases of the virgin specimen ('immediately before' CP) were greatly influenced by continuous creep deformation. The effect of creep was large at the vicinity of the lowest and the highest stress states during the CP stress cycle (i.e., the segments ef and gh of the unloading curve while ab and cd of the reloading curve). That is, due to this creep effect, the E_{tan} values observed immediately after reversing the loading direction (i.e., those near the point a and e) are noticeably larger than the respective elastic Young's modulus E_{max} measured under otherwise the same condition. E_{tan} value decreases

compared to the respective E_{max} value both with the increase in σ_a during reloading and with the decrease in σ_a during unloading. These results show that plastic strain increments take place similarly during reloading and unloading. Prestrained specimen, on the other hand, exhibits rather similar values of E_{tan} at a given σ_a for both reloading and unloading phases (the maximum difference was 10% in extension zone), while the difference between the corresponding E_{tan} and E_{max} values is much smaller than it is before CP. This is due to a substantial decrease in plastic strain increments during CP. Yet the average of unloading E_{tan} and reloading E_{tan} at a given σ_a along the CP stress cycle of the prestrained specimen was lower than the corresponding value of E_{max} by 15~24% of the average E_{tan}. It could be because of the presence of plastic strain component, though small, in the axial strain ε_a. Due to CP-induced anisotropy, the value of E_{tan} at a given σ_a of the prestrained specimen was lower than the corresponding value of the virgin specimen in spite of reduced plastic strain increments, except in some zone near the peak in compression side during reloading.

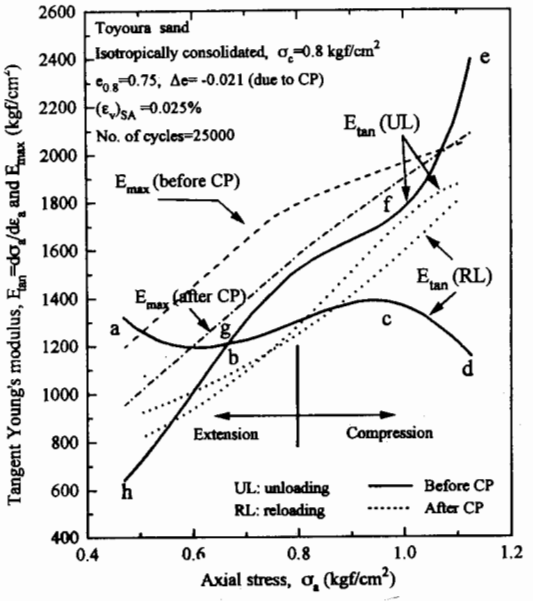

Fig 6. Variation of tangent moulus E_{tan} along the CP stress path (1 kgf/cm^2 = 98 kPa)

Effects of aging and CP on E_{max}

Figs. 7a and b show the variation of E_{max} (after corrected for the changes in void ratio) at σ_c equal to 0.8 kgf/cm^2 (78 kPa) for the entire time history of each experiment. Two specimens having void ratios $e_{0.8}$ =

0.75 and 0.65 were tested. The figures show : a) a marginal increase with time involving some scatter in E_{max} prior to CP application; b) a sudden drop (the maximum of about 20% in the looser specimen) of E_{max} by CP; c) partial recovery of Young's modulus in the initial part of post-CP consolidation period, followed by a very slow increase in E_{max} with time. [4]. In the tests, void ratio did not change largely as given in brackets in the respective figures.

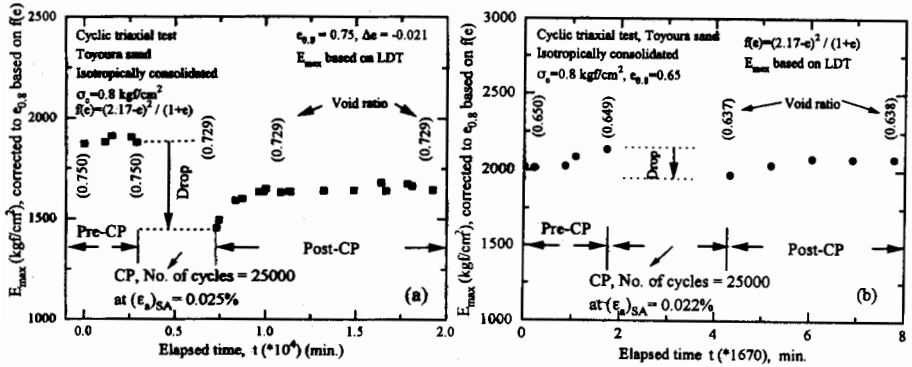

Fig 7. Variation of E_{max} at neutral stress (σ_c=0.8 kgf/cm^2) with time for (a) $e_{0.8}$=0.75, (b) $e_{0.8}$=0.65 (1 kgf/cm^2 = 98 kPa)

As mentioned earlier, the effects of CP on the E_{max} value is not consistent among different tests. Effects of the different degrees of cyclic prestraining on the E_{max} values obtained from another series of tests on Toyoura and Ticino Snads performed following the test procedure shown in Fig. 2b can be seen from Fig. 8. All the tests, except one on Ticino sand, were performed at an isotopic neutral stress state of either 0.8 kgf/cm^2 (78 kPa) or 0.5 kgf/cm^2 (49 kPa); one test on Ticino sand was performed at an anisotropic neutral stress state (K=σ_r/σ_a=0.4) with σ_r = 0.5 kgf/cm^2 (49 kPa). Table 1 shows the total changes in void ratio due to CP. The amount of densification by CP was very small for these relatively dense specimens. For the loose sepcimens, however, the changes in void ratios due to CP were noticeable. The variation of E_{max} (=$(E_{eq})_{max}$)/f(e) with the number of loading cycles applied during CP is shown in Fig. 8. It is clear to see that the effect of CP on the E_{max}, excluding the effect of densification, was very small.

Summarizing the above, it can at least be concluded that the E_{max} values does not change substantially due to CP applied at strains largely exceeding the elastic limit, and neither does the void ratio. Furthermore, E_{max} value does not increase at a very large rate under sustained long-term consolidation.

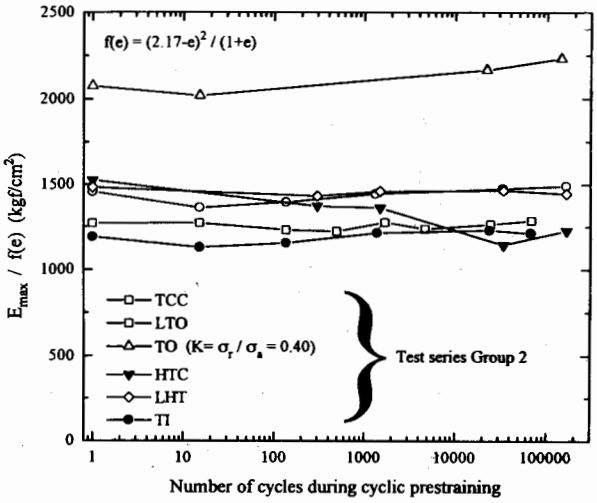

Fig 8. Plot between the E_{max} and the degree of prestraining for different speimens (1 kgf/cm² = 98 kPa)

CONCLUSIONS

Granular soil becomes anisotropic as a result of the application of a large amplitude cyclic axial loading for a large number of cycles (as called CP). CP was observed to affect the dependency on the axial stress σ_a of the elastic Young's modulus E_{max} defined based on very small increments of axial stress and strain. That is, the dependency of E_{max} on σ_a increases by CP. This kind of anisotropy may be called the CP-induced anisotropy. This could be associated with particle re-arrangement by sliding and rotation during CP, which may cause densification and damage as well. Therefore, E_{max} measured at the neutral stress state during CP was observed to be unstable, which varies in the range of 0.78~1.10 time the initial value depending on different specimens. Similar behaviour was observed on the decay curve between E_{eq} and $(\varepsilon_a)_{SA}$. An increase in the E_{max} value with elapsed time was observed during post-CP consolidation period, which means a gradual decrease in the effects of CP-induced anisotropy with time.

ACKNOWLEDGEMENT

The authors are grateful to Mr. Sato, T. and Dr. Kohata, Y. for their help during the research. The research is funded by the Ministry of Education, Science and Culture of Japan.

REFERENCES

Alarcon-Guzman, A., J.L. Chameau, G.A. Leonard and J.D. Frost (1980), "Shear Modulus and Cyclic Undrained Behaviour of Sands". *Soils and Foundations*, Vol. 20, No. 4, pp. 105-119.

De Alba, P., K. Baldwin, V. Janoo, G. Roe and B. Celikkol (1984)., "Elastic wave velocities and liquefaction potential". *Geotechnical Testing Journal*, ASTM, Vol. 7, No. 2, pp. 77-87.

Drnevich, V.P. and F.E. Richart (1970)., "Dynamic prestraining of dry sands". *J. of Soil Mechanics and Foundation Engg.*, ASCE, Vol. 96, No. SM2, 1970, pp. 451-469.

Hoque, E. F. Tatsuoka, and T. Sato (1995)., "Combined Effects of Cyclic Prestraining and Aging on Elastic Modulus of Dry Toyoura Sand". *Proc. 50th annual conf. of JSCE*, Matsuyama, Vol. 3, pp. 298-299.

Hoque, E. F. Tatsuoka, and T. Sato (1996), "Measuring Anisotropic Elastic Properties of Sand Using a Large Triaxial Specimen". Geotechnical Testing Journal, ASTM, Vol. 19, No. 4, pp. 411-420.

Hoque, E. F. Tatsuoka, T. Sato, and Y. Kohata (1995). "Inherent and Stress-induced Anisotropy in Small Strain Stiffness of Granular Materials". *First Int. Conf. on Earthquake Geotechnical Engg.*, IS-Tokyo, Vol. 1, pp. 277-282.

Flora, A., G.L. Jiang, Y. Kohata and F. Tatsuoka (1994). "Small Strain Behaviour of a Gravel along some Triaxial Stress Paths". *Proc. Int Symp. on Prefailure Deformation Characteristics of Geomaterials*, IS-Hokkaido '94, Balkema, Vol. 1, pp. 279-285.

Goto, S., F. Tatsuoka, S. Shibuya, Y.-S. Kim and T. Sato (1991), "A Simple Gauge for Local Small Strain Measurements in the Laboratory". *Soils and Foundations*, Vol. 31, No. 1, pp. 169-180.

Hardin, B.O. and V.P. Drnevich (1972), "Shear Modulus and Damping in Soils : Measurement and Parameter effects". *Jouranl of SMF Div.*, Proc. ASCE, Vol. 98, SM6, pp. 603-624.

Jamiolkowski, M., S. Lerouell and D.C.F. Lo Presti (1991), "Design Parameters from Theory to Practice". *Theme Lecture, Geo-Coast '91, Yokohama*, pp. 877-917.

Jardine, R.J., Symes, M.J.P.R., and Burland, J.B. (1984), "The Measurement of Soil Stiffness in Triaxial Apparatus". *Geotechnique*, Vol. 34, No. 3, pp. 323-340.

Stokoe, K.L.II., J.N.K. Lee and S.H.H. Lee (1991), "Characterization of Soil in Calibration Chambers with Seismic Waves", *Proc. of Int. Symp. on Calibration Chamber Testing*, Clarkson Univ., Postdam, NY (Huang ed.), Elsevier, pp. 363-376.

Tatsuoka, F. and Y. Kohata (1995), "Stiffness of Hard Soils and Soft soils in Engineering Applications. *Report of the Institute of Industrial Science*, The University of Tokyo, Vol. 38, Serial No. 242.

Tatsuoka, F., D.C.F. Lo Presti and Y. Kohata (1995), "Deformation Characterstics of Soils and Soft Rocks under Monotonic and Cyclic Loads and their Relationships", *Keynote Lecture, Proc. Int. Conf. on Recent Advances in Geotechnical Earthquake Engineering and Soil Dynamics (Prakash eds.)*, Vol. II, pp. 851-879.

Tokimatsu, K., T. Yamazaki and Y. Yoshimi (1986), "Soil liquefaction evaluations by elastic shear moduli". *Soils and Foundations*, Vol. 26, No. 1, pp. 25-35.